American Mineralogist, Volume 88, pages 93–98, 2003

Synthetic $MgAl_2O_4$ (spinel) at high-pressure conditions (0.0001–30 GPa): A synchrotron X-ray powder diffraction study

DAVIDE LEVY,[1,*] ALESSANDRO PAVESE,[2,3] AND MICHAEL HANFLAND[4]

[1]Dipartimento Scienze Mineralogiche e Petrologiche-Università degli Studi di Torino, Via Valperga Caluso 35, 10025 Torino, Italy
[2]Dipartimento Scienze della Terra, Università degli Studi di Milano, Via Botticelli 23, 20133 Milano, Italy
[3]National Research Council, IDPA, Section of Milan, Via Mangiagalli 34, 20133 Milano, Italy
[4]European Synchrotron Radiation Facility, ESRF, F 38043 Grenoble Cedex, France

ABSTRACT

The equation of state and the structural behavior of synthetic $MgAl_2O_4$ have been investigated using synchrotron X-ray powder diffraction data collected to 30 GPa at room temperature. The Birch-Murnaghan, Vinet, and Poirier-Tarantola models have been fitted to the observed *P*-*V* data. The Birch-Murnaghan equation of state, with V_0 fixed at its experimental value, yields $K_0 = 190.8(\pm 1.2)$ GPa, $K_0' = 6.77(\pm 0.15)$ and $K_0'' = -0.075$ GPa^{-1} (implied value). The compression of spinel occurs with a negligible change of the fractional coordinate of oxygen. Therefore the structural shrinking is a function of cell edge shortening alone. The results presented here are compared with those from the literature.

INTRODUCTION

Spinels (AB_2O_4, where A and B are, in most cases, divalent and trivalent cations, respectively; space group $Fd\bar{3}m$) have structures described by three symmetry-independent sites: a tetrahedral site (T), an octahedral site (M), and an O atom-bearing site [*u,u,u*]. The A and B cations are distributed over the T and M sites and undergo order-disorder reactions triggered by temperature (*T*) which have been extensively investigated [see, for example, Andreozzi et al. (2000), Redfern et al. (1999), and the references reported therein]. The cation partitioning in spinels allows one to speculate on the thermal path experienced by the samples, and hence spinels can be exploited as geo-thermometers and petrogenetic indicators (Sack 1982). The study of spinels at high pressure (*P*) is relevant for planetary interiors, given that the structure of these minerals is a model for phases which are stable under Earth mantle conditions; for this reason the behavior of spinels as a function of *P* has been the subject of several studies (Levy et al. 2001, 2000; Haavik et al. 2000; Fei et al. 1999; Funamori et al. 1998; Yutani et al. 1997).

Among spinels, $MgAl_2O_4$, i.e., spinel in sensu stricto (hereafter called simply spinel), is one of the most significant minerals of this group for geophysical purposes, as it is a constituent of the upper mantle of the Earth (Navrotsky 1994) and is believed to occur in subducted oceanic crust with the $CaFe_2O_4$-type structure (Kesson et al. 1994).

The study of the structural behavior of spinel at high pressure (*HP*) was first carried out by Finger et al. (1986), up to about 5 GPa. Subsequently Pavese et al. (1999) investigated spinel by neutron powder diffraction up to 4 GPa, paying particular attention to the cation partitioning.

Liu (1978), Irifune et al. (1991), and Funamori et al. (1998) pointed out that spinel undergoes transformations under pressure, though ambiguities persist about their nature.

O'Connell and Graham (1971), Chang and Barsch (1973), Liu et al. (1975), Yoneda (1990), Cynn (1992), and Askarpour et al. (1993) studied the elastic properties of $MgAl_2O_4$ by measuring the elastic constants.

The present study is devoted to investigating the equation of state and the structural behavior of spinel from ambient conditions to about 30 GPa by in situ high-pressure powder diffraction using X-rays from a synchrotron source, at room temperature. This investigation complements the previous studies by significantly extending the *P* interval explored such that the equation of state of this material can be properly stated, and so that an account of the structural response of spinel in the high-pressure regime can be given.

EXPERIMENTAL METHODS

Sample

The sample used in the present experiment was synthesized by heating a quasi-stoichiometric mixture of reagent grade MgO and Al_2O_3 (supplied by Carlo Erba SpA), with a slight excess of the former, for 18 hours at 1600 °C. The product of the reaction was first cooled to room temperature at a rate of ≈30 °C/hour, which took approximately three days, and then treated with dilute nitric acid to eliminate the residual MgO. A powder diffraction pattern collected with a laboratory diffractometer (X'PERT Phillips) confirmed the spinel structure and did not reveal any occurrence of the parent phases. The chemical composition of the synthesized spinel was determined by averaging 24 analyses performed with an ARLSEMQ electron microprobe, which yielded $Mg_{0.95(4)}Al_{2.03(3)}O_4$. The uncertainties reported take into account the propagation of errors in averaging.

The cation partitioning of the synthesized sample was determined using the approach of Lavina et al. (2002). This method is based on minimization of the differences between

* E-mail: alessandro.pavese@unimi.it

theoretical and observed crystal chemical parameters (interatomic distances and lattice edge) of spinel-like structures, using the chemical compositions as soft constraints. The theoretical crystal-chemical parameters are assumed to be linear functions of the occupancy factors and of "absolute" T-O and M-O bond distances. These parameters hold for any spinel and depend only on the chemical species. The calculation is carried out to fix the "absolute" X-O atoms and the cation partitioning using all the spinel structures studied to date, to warrant statistical reliability. Three schemes were tried. One assumed vacancies in M only, the second in T only, and the last was a defect free model; they all give an Al occupancy factor in the T site of 0.21(1) and produce comparable χ^2 values. Therefore, we were not able to definitely fix the vacancy distribution; note, however, that this is in keeping with the uncertainties in chemical composition, which are of the same magnitude as the vacancy concentrations.

High-pressure powder diffraction

The high-pressure powder diffraction experiment was carried out at ESRF (European Synchrotron Radiation Facility, Grenoble, France) on the ID9 beamline. The *HP* conditions were achieved by means of a DAC (diamond anvils with 300 μm diameter culets; hole in the gasket of 125 μm diameter), using N_2 as a pressure transmitting medium. A total of 28 patterns were recorded, up to 40 GPa; however, we only used the results from the first 22 data sets, neglecting those above 30 GPa, which show broad and asymmetric diffraction peaks and therefore suggest a structural transformation in progress. The shift of the fluorescence line of ruby excited by an Ar laser source was adopted to determine *P* according to the non-linear hydrostatic pressure scale of Mao et al. (1986). The uncertainty on *P* [$\sigma(P)$] was fixed at 0.1 GPa as in several previous works based on data collected at ID9 (Pavese et al. 2001; Levy et al. 2001; Levy et al. 2000), because it was observed that $\sigma(P) \approx$ 0.1 GPa is consistent with the χ^2 values (i.e., $\chi^2 \approx 1$) attained by fitting EoS models to the measured *P*. The crystallization of N_2 poses serious problems, in particular at elevated pressures, as it causes non-hydrostaticity in the *HP* chamber (Duffy and Wang 1998), which makes it difficult to fix *P* values. N_2 has three different solid phases at high pressure and room temperature (Olijnyk 1990): the β-N_2 phase, between about 1 and 2 GPa, with disordered hexagonal structure, the δ-N_2 phase, between 2 and 11 GPa, with disordered cubic structure, and the ε-N_2 phase above 11 GPa, with ordered rhombohedral structure. The bulk elastic properties for the β phase are not reported, while δ and ε phases exhibit bulk moduli of 2.69 and 2.98 GPa, respectively. Non-hydrostaticity can be corrected for by annealing the *HP* environment. As the *HP* cell we used did not allow heating, we corrected *a posteriori* the experimental pressures using a function (ΔP) defined as $\Delta P = 0$ if $P < P_0$, and $\Delta P = w_0 + w_1 P$, if $P > P_0$. The values of w_0 (≈0.2 GPa), w_1 (≈0.0 GPa^{-1}), and P_0 (≈20 GPa) were determined to (1) decrease the initial χ^2 value (i.e., 1.5) to unity, and (2) improve of consistency between the values of the bulk modulus and its first derivative vs. *P* attained by the third order Birch-Murnaghan EoS refining V_0 or keeping it fixed at its experimental value. Note that (1) the form we have chosen for ΔP can be assumed as a Taylor expansion of a more complex corrective function, and (2) $w_1 \approx 0$ GPa^{-1} suggests no *P*-dependent contribution for the correction of pressure is significant. For this reason we did not try to model ΔP with higher order polynomials in *P*. ΔP accounts for errors affecting V_0 and *P*. In the present case, however, V_0 is reliably measured, as discussed at the end of this section and confirmed by the results obtained by refining V_0; therefore we assume ΔP to be reflective of the deviations on *P* only. The use of an internal standard is more appropriate in accounting for deviations in pressure, but results in a serious hindrance if one intends to carry out structure refinements on the basis of powder diffraction patterns.

The X-ray beam from the U46 undulator was focused vertically with a Pt-coated Si mirror and horizontally with an asymmetrically cut bent Si(111) Laue monochromator to a spot ~30 × 30 μm^2. Diffraction images were collected at a wavelength of $\lambda = 0.47954$ Å, calibrated with NBS silicon; sample to plate distance was 541.578 mm resulting in an angular resolution of about 0.04°. The image plate was scanned with a 100 μm resolution Molecular Dynamics STORM Image Plate Reader. Data collection required about 20 min in total. The two-dimensional images were integrated with FIT2D (Hammersley et al. 1996) into one-dimensional diffraction patterns; we then used the GSAS software package (Larson and Von Dreele 1986) to perform Rietveld structure refinements. The experimental patterns were satisfactorily modeled by pseudo-Voigt profile functions, whose Full Width at Half Maximum (FWHM) was parametrized as $\sigma^2 = \sigma_0 \tan(\theta)^2$ and $\gamma = \gamma_0/\cos(\theta)$, in terms of Gaussian and Lorenzian components, respectively. The background was accounted for by means of a 20 term cosine-function expansion; the resulting peak asymmetry was negligible. The diffraction pattern regions where the most intense peaks of crystalline N_2 occur were excluded from the profile treatment.

Equilibrium at given *P* was assumed to be achieved if on monitoring pressure every fifth minute no variation larger than 0.03 GPa was observed. This procedure required a mean time of 30 minutes for each *P* point.

In Figure 1 the diffraction pattern at 12.4 GPa is shown. The lattice parameter (*a*), the O atom coordinate (*u*), the isotropic atomic displacement parameters, the background coefficients, and the FWHM parameters were refined. The

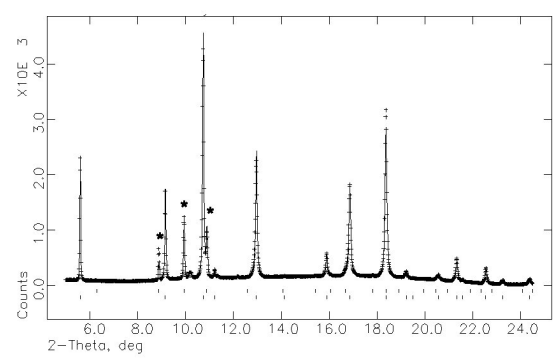

FIGURE 1. Experimental (crosses) and calculated (full line) powder diffraction patterns of synthetic spinel at 12.4 GPa; the residual curve and peak position markers are shown. Stars show the peak positions of crystalline N_2.

parameters a and u are given in Table 1. The lattice parameter is plotted as a function of P in Figure 2; the a values were fitted by a third order polynomial ($a_0 + a_1P + a_2P^2 + a_3P^3$), with coefficients a_0 = 8.0812(2) Å, a_1 = –0.0139(2) Å GPa^{-1}, a_2 = 0.00022(2) Å GPa^{-2} and a_3 = –0.0000027(9) Å GPa^{-3}. Note that a at room conditions was measured first outside (see value in Table 1), and then inside the *HP* cell without load, and full agreement was observed; such determinations also agree with that obtained using the polynomial equation above.

Results and discussion

Equation of state

The bulk elastic properties of spinel were investigated by fitting the Birch-Murnaghan EoS (Birch 1986), the Vinet EoS (Vinet et al. 1987, 1986), and the Poirier-Tarantola EoS (Poirier and Tarantola 1998) to the measured pressure values. The Birch-Murnaghan model results in

$$P(V) = 3K_0f_E(1 + 2f_E)^{5/2}(1 + Af_E + Bf^2_E) \quad (1)$$

where K_0 is the bulk modulus at P = 0, $A = 3/2(K'_0 - 4)$, and $B = 3/2[K_0K''_0 + (K'_0 - 4)(K'_0 - 3) + 35/9]$, with K'_0 and K''_0 corresponding to the first and second derivatives of K vs. P at ambient conditions (i.e., at 0.0001 GPa; hereafter indicated as P = 0, for the sake of brevity); f_E is the Eulerian strain defined as follows

$$f_E = [(V_0/V)^{2/3} - 1]/2 \quad (2)$$

where V_0 and V stand for the volume at P = 0 and at a given pressure, respectively. The Vinet EoS is expressed as

$$P(V) = 3K_0 \frac{(1 - f_V)}{f_V^2} \exp\left[\eta(1 - f_V)\right] \quad (3)$$

where $\eta = 3/2(K'_0 - 1)$ and $f_V = (V/V_0)^{1/3}$. The Poirier-Tarantola EoS calculates pressure as

$$P(V) = 3K_0\left(\frac{V_0}{V}\right) f_N\left(1 + Af_N + Bf_N^2\right) \quad (4)$$

where $A = 3/2(K'_0 - 2)$, $B = 3/2[1 + K_0K''_0 + (K'_0 - 2) + (K'_0 - 2)^2]$, and f_N is defined as $f_N = 1/3 \ln(V_0/V)$.

In Figures 3a and 3b graphs of the normalized pressures P_{bm} as a function of f_E {P_{bm}=$P/[3 f_E(1 + 2 f_E)^{5/2}]$} and P_{pt} as a function of f_N {P_{pt}=$P/[3 f_N](V/V_0)$} are shown, respectively; these suggest that third-order expansions of Equations 1 and 4 are sufficient to treat the present P-V data. Table 2 gives the values of the bulk elastic properties determined by the EoSs presented above; previous measurements of K_0 are also reported. Note that the discussion which follows refers to the elastic properties obtained using pressure corrected as explained in the previous section.

We first discuss the self consistency of the results obtained by different EoS models (BM3, BM4, V, PT3, PT4; acronyms explained in the caption to Table 2), and then compare our K_0 and K'_0 with earlier determinations. For the sake of completeness we also explore the effects on the elastic properties of refining V_0, although this value should be assumed to be known and set to its experimental value. Note that the EoS models do not yield significant differences in terms of χ^2.

All of the models presented give elastic properties that are modestly sensitive to the refinement of the volume at ambient conditions. K_0 and K'_0 determined by refining V_0 vary within 1σ from the values obtained by keeping V_0 fixed at the experimental value. The refined V_0 also does not differ by more than 1σ from the experimental value. We observe that the greatest changes between the elastic parameters determined at fixed V_0 and those attained by refining V_0 occur in the case of the fourth

Table 1. Results from structure Rietveld refinements: lattice parameter (Å) and u coordinate of oxygen for spinel

P(GPa)	a (Å)	u	$R(F^2)$	R_{wp}
0.0	8.08149(1)	0.26262(6)	4.1	3.4
0.6(1)	8.07262(1)	0.26265(2)	3.6	1.1
1.1(1)	8.06652(2)	0.26261(2)	7.6	1.6
1.7(1)	8.05714(2)	0.26195(4)	5.1	1.6
3.1(1)	8.04100(2)	0.26260(4)	10.2	2.4
4.5(1)	8.02441(7)	0.26251(9)	19.6	3.6
5.0(1)	8.01530(5)	0.26192(18)	15.2	3.2
5.9(1)	8.00560(7)	0.26227(19)	19.2	3.6
7.2(1)	7.98909(9)	0.26226(21)	4.2	5.2
8.1(1)	7.98193(7)	0.26215(15)	4.2	3.2
9.1(1)	7.97068(7)	0.26251(12)	2.9	3.5
10.1(1)	7.96121(8)	0.26303(10)	7.4	3.1
11.1(1)	7.94976(9)	0.26239(12)	3.9	3.6
12.4(1)	7.93731(9)	0.26240(17)	4.7	3.7
13.9(1)	7.92235(11)	0.26249(13)	11.3	3.5
15.6(1)	7.90729(11)	0.26295(15)	6.9	3.9
17.0(1)	7.89371(14)	0.26298(13)	12.7	2.8
18.5(1)	7.88263(20)	0.26222(13)	30.4	4.8
20.2(1)	7.86493(18)	0.26208(18)	21.0	3.6
22.6(1)	7.84685(27)	0.26299(7)	18.5	4.0
25.1(1)	7.82825(24)	0.26221(12)	21.7	4.0
29.0(1)	7.79994(26)	0.26220(11)	10.9	3.8

Notes: $R(F^2)$ = sqrt[$\Sigma^{\circ} F_o^2 - F_c^{2\circ} / \Sigma F_o^2$]×100. R_{wp} = sqrt[$\Sigma(I_o - I_c)^2 w$], where w = weighting factor. The P values shown have been corrected as explained in the text.

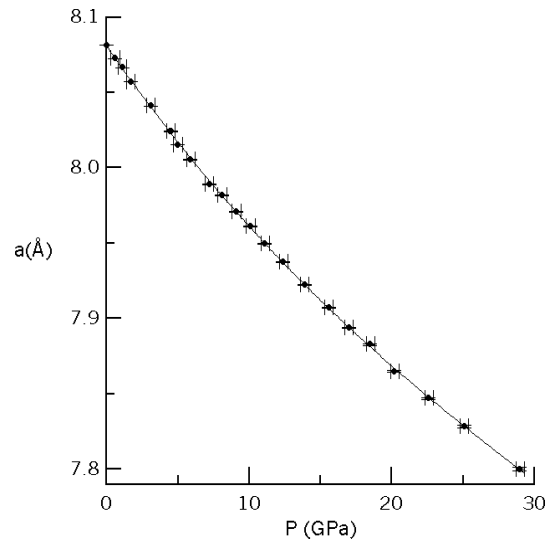

Figure 2. Cell edge (Å) as a function of pressure (GPa). The solid line is the third order polynomial fit.

TABLE 2. Bulk modulus (K_0), its first (K_0') and second (K_0'') derivatives with respect to pressure, and cell volume (V_0) at room conditions, according to the EoSs of Birch-Murnaghan, Vinet, and Poirier-Tarantola

	K_0 (GPa)	K_0'	K_0'' (GPa^{-1})	V_0 (Å^3)	χ^2
Results obtained from *P* values determined using ruby and corrected as explained in the text					
BM3	190.8(±1.2)	6.77(±0.15)	–0.075	527.8059	0.98
BM3v	191.2(±2.5)	6.73(±0.21)	–0.074	527.78(±0.14)	1.03
BM4	191.4(±3.1)	6.56(±0.90)	–0.05(±0.09)	527.8059	1.04
BM4v	193.2(±5.6)	6.24(±1.20)	–0.01(±0.12)	527.74(±0.18)	1.08
V	190.8(±1.2)	6.78(±0.15)		527.8059	0.98
Vv	191.1(±2.4)	6.75(±0.22)		527.78(±0.14)	1.03
PT3	188.6(±1.3)	7.56(±0.18)	–0.199	527.8059	1.02
PT3v	188.0(±2.8)	7.61(±0.26)	–0.203	527.84(±0.15)	1.07
PT4	191.4(±3.3)	6.53(±1.01)	–0.03(±0.12)	527.8059	1.04
PT4v	193.2(±5.9)	6.18(±1.35)	0.01(±0.15)	527.74(±0.18)	1.09
Results obtained from *P* values determined using ruby					
BM3	192.2(±1.5)	6.44(±0.19)	–0.064	527.8059	1.53
BM3v	193.2(±3.1)	6.36(±0.26)	–0.061	527.74(±0.18)	1.60
BM4	192.4(±3.9)	6.39(±1.13)	–0.06(±0.12)	527.8059	1.61
BM4v	195.1(±6.9)	5.90(±1.50)	–0.01(±0.14)	527.70(±0.22)	1.69
V	192.1(±1.5)	6.48(±0.19)		527.8059	1.53
Vv	192.9(±3.0)	6.42(±0.27)		527.75(±0.18)	1.60
PT3	190.2(±1.6)	7.16(±0.22)	–0.1721	527.8059	1.55
PT3v	190.3(±3.4)	7.14(±0.31)	–0.1709	527.79(±0.19)	1.63
PT4	192.2(±4.2)	6.43(±1.26)	–0.06(±0.15)	527.8059	1.62
PT4v	194.8(±7.4)	5.90(±1.67)	–0.01(±0.18)	527.71(±0.22)	1.69
Previous results from the literature					
			Technique		
PAH	190(±2)	4.0	HP powder diffraction		
AMFY	200(±3.4)		Brillouin spectroscopy		
Y	197.9		Ultrasonic method		
FHH	194(±6)	4.0	HP single crystal diffraction		
LSA	196.9		Light-sound scattering		
CB	197.4		Ultrasonic method		
OCG	197.5		Ultrasonic method		

Notes: K_0'' values reported without uncertainties are implied values. BM3 = Third order Birch-Murnaghan EoS; BM3v = Third order Birch-Murnaghan EoS with refined V_0; V = Vinet model; Vv = Vinet model with refined V_0; PT3 = Third order Poirier-Tarantola EoS; PT3v = Third-order Poirier-Tarantola EoS with refined V_0. χ^2 = sqrt[$\Sigma(P_{obs} - P_{calc})^2/\sigma_t^2$]/($N - M$), where N = number of pressure points, M = degrees of freedom; σ^t = sqrt[$\sigma(P)^2 + (fP/fV)^2\sigma(V)^2$]. PAH: Pavese et al. (1999) (neutron powder diffraction at HP); AMFY = Askarpour et al. (1993) (Brillouin spectroscopy); Y = Yoneda (1990) (ultrasonic method); FHH = Finger et al. (1986) (X-ray single crystal diffraction at HP); CB = Chang and Barsch (1973) (ultrasonic method); LSA = Liu et al. (1975) (light-sound scattering); OCG = O'Connell and Graham (1971) (ultrasonic method).

order expansions (compare BM4 with BM4v, and PT4 with PT4v; discrepancies from 1% to 6%). Such a result is likely to be an effect of the correlations between the bulk modulus and its derivatives vs. P and V_0. We have an excellent consistency between the results from BM3 and BM3v, PT3 and PT3v, V and Vv (discrepancies confined within 0.7%). Altogether, these considerations suggest that discussion should be restricted to the elastic parameters in Table 2 obtained by models that do not refine V_0.

BM3 and V yield virtually the same elastic parameters, while PT3 gives K_0 and K_0' differing by more than 1σ from the solutions of the other models. The fourth order truncations, both in the case of the Birch-Murnaghan model and of the Poirier-Tarantola EoS, lead to K_0'' parameters less than 1σ different, consistent with expectations from Figures 3a and 3b, and to K_0 and K_0' values affected by greater uncertainties than those from BM3, PT3, and V. Whereas BM4 gives elastic parameters in basic agreement with those attained by BM3 (in keeping with $K_0'' < 1\sigma$), PT4 yields K_0 and K_0' values more than 1σ discrepant with the issues of PT3, and close to those of BM4. Such a result is consistent with the conclusions of Pavese (2002), who proved by fitting synthetic P-V-T data with the EoS models discussed here that PT3 systematically underestimates K_0 and overestimates K_0', while PT4 is more effective in reproducing the correct elastic parameters. Therefore the Birch-Murnaghan model seems less sensitive to truncation than the Poirier-Tarantola EoS, in agreement with Poirier and Tarantola (1998), who claim a more regular convergence of the series (4) than of the expansion (1), as f_E changes more quickly than f_N with increasing P. If we calculate the bulk modulus at room pressure using the compressibility determined by the third-order polynomial fit reported in the previous section, K_0 = 193(±2) GPa is obtained, in reasonable agreement with the values determined via EoSs.

A comparison between the elastic parameters in Table 2 and in previous results reveals that K_0s determined by ultrasonic measurements or by Brillouin scattering are systematically larger than ours, which in turn agree within 1σ with the values obtained by high-pressure diffraction experiments. The narrow P-ranges explored by Finger et al. (1986) and by Pavese et al. (1999) prevented those authors from determining K_0', which was kept at 4, i.e., B = 0 in Equation 1. Had we set K_0 = 196 GPa and refined K_0', BM3 would yield K_0' = 6.09 (±0.05) and χ^2 = 1.8; this demonstrates that the present P-V data do not match an EoS model based on a bulk modulus value close to the ones determined previously by ultrasonic methods or Brillouin light scattering. Such a disagreement might be attributed to the differences between measurements of adiabatic (by ultrasonic and

Brillouin light scattering) and isothermal bulk modulus (by EoSs), and to the uncertainties in the thermodynamic quantities used to convert K_S into K_T. If we used the raw P values, that is without the correction mentioned in the Experimental section, we would get slightly different elastic properties (discrepancies within 2σ, see Table 2) but with larger uncertainties and χ^2 values (≈1.5).

The use of the confidence ellipses (Bass et al. 1981) does not add further contributions to the analysis of the results of Table 2 with respect to the discussion above.

In the case of synthetic $ZnAl_2O_4$, Levy et al. (2001) obtain $K_0 = 201.7$ (±0.9) GPa and $K_0' = 7.62$ (±0.09), by BM3 at fixed V_0. This suggests that the replacement of Zn with Mg leads to a decrease of the bulk modulus at $P = 0$, against expectations based on the cation size. However, note that in gahnite one finds a quasi-normal structure, whereas in the present case a significant degree of inversion occurs [0.21(1), see the Experimental section], and that vacancies play an important role in affecting the physical properties of materials (Viertel and Seifert 1979).

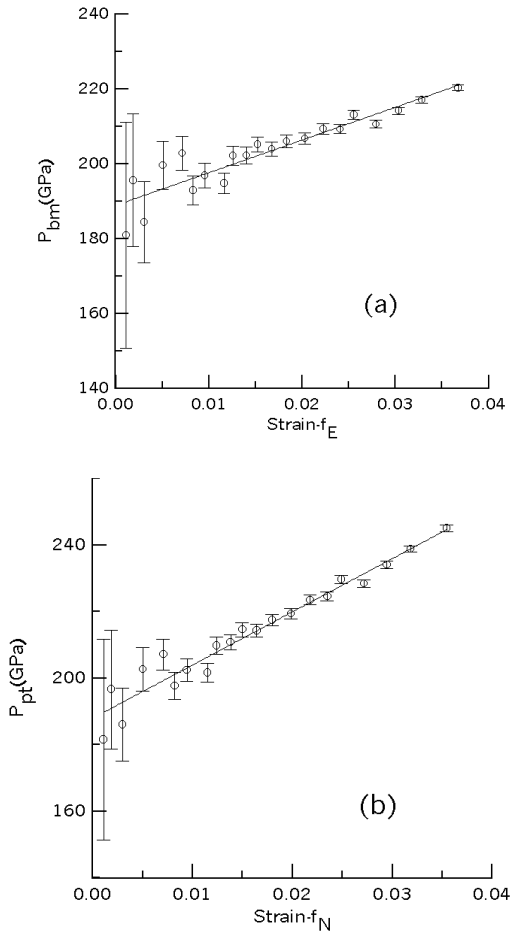

FIGURE 3. Normalized pressures P_{bm} (**a**) and P_{pt} (**b**), defined in the text, vs. strain.

Structure at high pressure

The structure of spinels is fully described by only one independent positional variable for O atoms, i.e., u. It is straightforward to prove that the bond-length compressibilities and the polyhedral volume compressibilities (β^X where X corresponds to a bond length or to a polyhedral volume) can be split into two parts (Nakagiri et al. 1986); one is dependent only on a (β_a^X) and the other is a function of u alone (β_u^X). The latter, in turn, is factorized into two parts, one of which is $(\partial u/\partial P)$. Figure 4 shows the behavior of u as a function of P; note that, aside from statistical oscillations, u exhibits a practically flat trend. If a linear function, i.e., $u_0 + u_1P$, is fitted to the observed u values using $1/\sigma(u)^2$ values as weights one obtains $u_0 = 0.2625(1)$ and $u_1 = 0.9(8.9)\ 10^{-6}$ GPa^{-1}, compared to those calculated using the u values of Finger et al. (1986) [u_1=-0.11(6) 10^{-3} GPa^{-1}] and Pavese et al. (1999) [u_1= 0.24(2) 10^{-3} GPa^{-1}]. Note that both the quoted studies report few pressure points (5 and 6 respectively) collected over narrow P intervals, not exceeding 5 GPa. These aspects may be a hindrance to fixing a reliable u_1 given that (1) oscillations frequently affect the results from *HP* measurements and many pressure points are needed to provide statistical reliability, and (2) spinels are compounds with generally large bulk moduli and therefore require a wide pressure range to fully reveal their compression mechanisms. Pavese et al. (1999) claim an Al/Mg order-disorder reaction is triggered by P in the low-pressure regime, supported by refinements of site occupancies. The possibility of investigating Mg/Al partitioning in the same way is beyond the scope of the present data, which do not allow one to reliably discriminate between Mg and Al (quasi-isoelectronic species), nor do we observe any evidence of discontinuity of the cation-O atom bond lengths as a function of pressure that might hint an atomic readjustment.

It is important in the present case to analyze the oscillations that affect the u values to understand whether the flat trend of the O atom coordinate is reflective of the actual physical be-

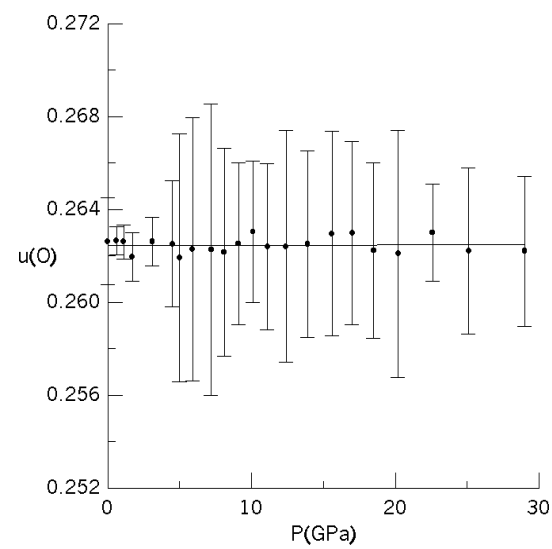

FIGURE 4. u as a function of pressure (GPa). Error bars correspond to 3σ.

havior of spinel, or is just a consequence of insufficient precision. If one uses the u_1 values from Pavese et al. (1999) and from Finger et al. (1986) to extrapolate u to 30 GPa, the absolute shifts of u from the values at ambient conditions are about 0.007 and 0.003, respectively. Our u values are scattered around a mean value by ±0.0003 (calculated as the variance of the u values in Table 1), which is significantly smaller than the expected changes due to pressure. On this basis we claim that β_u^X is of negligible import, as $\partial u/\partial P \approx 0$, and the structural behavior of spinel under compression is mainly governed by shrinkage of the cell edge. Hence, P acts upon $MgAl_2O_4$, producing a scaling of the structure. β^T and β^M are therefore equal to each other, being dependent on β_a^X only, and correspond to $1/K_0$, i.e., 0.00524(3) GPa^{-1} according to BM3, at $P = 0$. Finger et al. (1986) report $\beta^T = 0.008(1)$ GPa^{-1} and $\beta^M = 0.0038(6)$ GPa^{-1}. Note, however, that u_1 from those authors is determined at the 2σ level of significance, and therefore the site elastic properties are modestly reliable in terms of their u-dependent components, which are responsible for the different behaviors of the tetrahedra and octahedra.

The discrepancies we have with Finger et al. (1986) might be caused by a different degree of inversion in the samples used. It is something of a mystery that there is disagreement between our u_1 (≈ 0), and that of Pavese et al. (1999), i.e., (>0), because the latter resulted from a sample with a degree of inversion of 0.17, very close to that of the present spinel. Leaving out any explanation invoking differences in chemical composition, which although present are too small to be reasonably responsible for the disagreement, we propose to take into account the fact that the samples used are both synthetic, and therefore bear a variety of extended defects (planar defects, clustering, etc.) that can affect the position of O atoms in the structure. This is even more likely given that the present experiment was performed without thermal treatment (annealing), which speeds up relaxation of atoms into their equilibrium position at given pressure.

ACKNOWLEDGMENTS

A.P. is indebted to A Della Giusta who determined the magnesium/aluminum partitioning at ambient conditions and reviewed the manuscript before submission. The European Synchrotron Radiation Facility is kindly acknowledged. The authors are grateful to J. Bass and an anonymous referee for providing valuable suggestions and comments.

REFERENCES CITED

Andreozzi, G.B., Princivalle, F., Skogby, H., and Della Giusta, A. (2000) Cation ordering and structural variations with temperature in $MgAl_2O_4$ spinel: an X-ray single crystal study. American Mineralogist, 85, 1164–1171.

Askarpour, V., Manghnani, M.H., Fassbender, S., and Yoneda, A. (1993) Elasticity of single-crystal $MgAl_2O_4$ spinel up to 1273 K by Brillouin spectroscopy. Physics and Chemistry of Minerals, 19, 511–519.

Bass, J.D., Liebermann, R.C., Weidner, D.J., and Finch, S.J. (1981) Elastic properties from acoustic and volume compression experiments. Physics of the Earth and Planetary Interiors, 25, 140–158.

Birch, F. (1986) Equation of state and thermodynamic parameters on NaCl to 300 kbar in the high temperature domain. Journal of Geophysical Research, 91, 4949–4954.

Chang, Z.P. and Barsch, G.R. (1973) Pressure dependence of single-crystal elastic constants and anharmonic properties of spinel. Journal of Geophysical Research, 78, 2418–2433.

Cynn, H. (1992) Effects of cation disordering in $MgAl_2O_4$ spinel on the rectangular parallelepiped resonance and Raman measurements of vibrational spectra. Ph.D. thesis, 169 p. University of California Los Angeles, Los Angeles.

Duffy, T.S. and Wang, Y. (1998) Pressure-volume-temperature equations of state. In R.J. Hemley, Ed., Ultrahigh-pressure mineralogy, p. 425–457. Reviews in Mineralogy, Mineralogical Society of America, Washington, D.C.

Fei, Y., Frost, D.J., Mao, H.K., Prewitt, C.T., and Häusermann, D. (1999) In situ structure determination of the high pressure phase of Fe_3O_4. American Mineralogist, 84, 203–206.

Finger, L.W., Hazen, R.M., and Hofmeister, A.M. (1986) High pressure crystal chemistry of spinel ($MgAl_2O_4$) and magnetite (Fe_3O_4): comparison with silicate spinels. Physics and Chemistry of Minerals, 13, 215–220.

Funamori, N., Jeanloz, R., Nguyen, H., Kavner, A., Cadwell, W.A., Fujino, K., Miyajima, N., Shinmei, T., and Tomioka, N. (1998) High pressure transformations in $MgAl_2O_4$. Journal of Geophysical Research, 103, 20813–20818.

Haavik, C., Stølen, S., Fjellvåg, H., Hanfland, M., and Häusermann, D. (2000) Equation of state of magnetite and its high-pressure modification: thermodynamics of the Fe-O system at high pressure. American Mineralogist, 85, 514–523.

Hammersley, A.P., Svensson, S.O., Hanfland, M., Fitch, A.N., and Häusermann, D. (1996) Two-dimensional detector software: from real detector to idealised image or two-theta scan. High Pressure Research, 14, 235–248.

Irifune, T., Fujino, K., and Ohtuni, E. (1991) A new high-pressure form of $MgAl_2O_4$, Nature, 349, 409–411.

Kesson, S.E., Fitz Gerald, J.D., and Shelley, J.M.G. (1994) Mineral chemistry and density of subducted basaltic crust at lower mantle pressures, Nature, 372, 767–769.

Larson, A.C. and Von Dreele, R.B. (1986) GSAS: General Structure Analysis System. Los Alamos National Laboratory, Report LAUR: 86–87.

Lavina, B., Salviulo, G., and Della Giusta, A. (2002) Cation distribution and structure modeling of spinel solid solutions. Physics and Chemistry of Minerals, 29, 10–18.

Levy, D., Pavese, A., and Hanfland, M. (2000) Phase transition of synthetic zinc ferrite spinel ($ZnFe_2O_4$) at high pressure, from synchrotron X-ray powder diffraction. Physics and Chemistry of Minerals, 27, 638–644.

Levy, D., Pavese, A., Sani, A., and Pischedda, V. (2001) Behaviour of synthetic $ZnAl_2O_4$ (gahnite) at high pressure conditions, from synchrotron X-ray powder diffraction. Physics and Chemistry of Minerals, 28, 612–618.

Liu, L.G. (1978) A new high pressure phase of spinel. Earth Planetary Science Letters, 41, 398–404.

Liu, H.P., Schock, R.N., and Anderson, D.L. (1975) Temperature dependence of single crystal spinel elastic constants from 293 to 423 K measured by light-sound scattering in the Raman-Nath region. Geophysical Journal of the Royal Astronomic Society, 42, 217–250.

Mao, H.K., Xu, J., and Bell, P.M. (1986) Calibration of the ruby pressure gauge to 800 kbar under quasi-hydrostatic conditions. Journal of Geophysical Research, 91, 4673–4676.

Nakagiri, N., Manghnani, M.H., Ming, L.C., and Kimura, S. (1986) Crystal structure of magnetite under pressure. Physics and Chemistry of Minerals, 13, 238–244.

Navrotsky, A. (1994) Physics and Chemistry of Earth materials. Cambridge University Press, U.K.

O'Connell, R.J. and Graham, E.K. (1971) Equation of state of stoichiometric spinel to 10 kbar and 800 K. Transactions of the American Geological Union, 52, 359.

Olijnyk, H. (1990) High-Pressure X-Ray-Diffraction Studies on Solid N_2 up to 43.9 GPa. Journal of Chemical Physics, 93, 8968–8972.

Pavese, A. (2002) Pressure volume temperature equations of state: a comparative study based on numerical simulations. Physics and Chemistry of Minerals, 29, 43–51.

Pavese, A., Artioli, G., and Hull, S. (1999) Cation partitioning vs. pressure in $Mg_{0.94}Al_{2.04}O_4$ synthetic spinel, by in situ powder neutron diffraction. American Mineralogist, 84, 905–912.

Pavese, A., Levy, D., and Pischedda, V. (2001) Elastic properties of andradite and grossular, by synchrotron X-ray diffraction at high pressure conditions. European Journal of Mineralogy, 13, 929–937.

Poirier, J.P. and Tarantola, A. (1998) A logarithmic equation of state. Physics of the Earth and Planetary Interiors, 109, 1–8.

Redfern, S.A.T., Harison, R.J., O'Neill, St.C.H., and Wood, D.R.R. (1999) Thermodynamic and kinetics of cation ordering in $MgAl_2O_4$ synthetic spinel up to 1600° from in situ neutron diffraction. American Mineralogist, 84, 299–310.

Sack, R.O. (1982) Spinels as petrogenetic indicators: activity composition relations at low pressures. Contributions to Mineralogy and Petrology, 79, 169–186.

Viertel, H.U. and Seifert, F. (1979) Thermal stability of defect spinels in the system $MgAl_2O_4$-Al_2O_3. Neues Jahrbuch fur Mineralogie Abhandlungen, 134, 167–182.

Vinet, P., Ferrante, J., Smith, J.R., and Rose. J.H. (1986) A universal equation of state for solids. Journal of Physics C: Solid State, 19, L467–L473.

Vinet, P., Smith, J.R., Ferrante, J., and Rose, J.H. (1987) Temperature effects on the universal equation of state of solids. Physical Review B, 35, 1945–1953.

Yoneda, A. (1990) Pressure derivatives of elastic constants of single crystal $MgAl_2O_4$. Journal Physics of the Earth, 38, 19–55.

Yutani, M., Yagi, T., Yusa, H., and Irifune, T. (1997) Compressibility of calcium ferrite-type $MgAl_2O_4$. Physics and Chemistry of Minerals, 24, 340–344.

MANUSCRIPT RECEIVED DECEMBER 4, 2001
MANUSCRIPT ACCEPTED SEPTEMBER 25, 2002
MANUSCRIPT HANDLED BY ALISON R. PAWLEY